Geohazard Mechanics 2 (2024) 37–48

Contents lists available at ScienceDirect

Geohazard Mechanics

journal homepage: www.keaipublishing.com/en/journals/geohazard-mechanics

A stacked multiple kernel support vector machine for blast induced flyrock prediction

Ruixuan Zhang [a], Yuefeng Li [b], Yilin Gui [a,c,d,*], Danial Jahed Armaghani [e], Mojtaba Yari [f]

[a] School of Civil and Environmental Engineering, Queensland University of Technology, Gardens Point, QLD, 4000, Australia
[b] School of Computer Science, Queensland University of Technology, Gardens Point, QLD, 4000, Australia
[c] Centre for Materials Science, Queensland University of Technology, Gardens Point, QLD, 4000, Australia
[d] Centre for Sustainable Engineered Construction Materials, Queensland University of Technology, Gardens Point, QLD, 4000, Australia
[e] School of Civil and Environmental Engineering, University of Technology Sydney, Ultimo, NSW, 2007, Australia
[f] Department of Mining Engineering, Faculty of Engineering, Malayer University, Malayer, 65719-95863, Iran

ARTICLE INFO

Keywords:
Multiple kernel learning
Support vector machine
Stacked model
Flyrock prediction

ABSTRACT

As a widely used rock excavation method in civil and mining construction works, the blasting operations and the induced side effects are always investigated by the existing studies. The occurrence of flyrock is regarded as one of the most important issues induced by blasting operations, since the accurate prediction of which is crucial for delineating safety zone. For this purpose, this study developed a flyrock prediction model based on 234 sets of blasting data collected from Sugun Copper Mine site. A stacked multiple kernel support vector machine (stacked MK-SVM) model was proposed for flyrock prediction. The proposed stacked structure can effectively improve the model performance by addressing the importance level of different features. For comparison purpose, 6 other machine learning models were developed, including SVM, MK-SVM, Lagragian Twin SVM (LTSVM), Artificial Neural Network (ANN), Random Forest (RF) and M5 Tree. This study implemented a 5-fold cross validation process for hyperparameters tuning purpose. According to the evaluation results, the proposed stacked MK-SVM model achieved the best overall performance, with RMSE of 1.73 and 1.74, MAE of 0.58 and 1.08, VAF of 98.95 and 99.25 in training and testing phase, respectively.

1. Introduction

Among all the rock excavation methods, the most effective one is still the blasting technique. During detonation of explosives in the blast hole, huge explosive energy is generated in the form of shock waves, leading to rock displacement and fragmentation [1]. However, only 20%~30% of the explosive energy can be utilized, and the remaining of this energy is wasted to surrounding environment, resulting in several negative effects such as ground vibration, air overpressure and flyrock [2–9]. Among these hazards, flyrock is considered as the main contributing factor of human injuries and structural damages [10,11]. The flyrock phenomenon is defined as a free rock particle generated by detonation that travels considerable distance away from the blast face. Main mechanisms leading to flyrock are identified as cratering, rifling and face bursting [12,13]. According to the existing studies, the influencing factors of flyrock can be divided into two types, including blast design parameters and rock properties, which are also called controllable and uncontrollable factors. As for blast design parameters, they are controllable since they can be modified by blasting engineers [14,15]. Burden, spacing, powder factor, hole diameter and stemming are all controllable parameters affecting the flyrock. The rock properties like RQD, tensile strength and Poisson's ratio are uncontrollable, as they depend on the site condition of blasting area and cannot be changed by human. Prediction of flyrock distance is key to manage and minimize the environmental damages of blasting. To address this issue, many researches were carried out to study the relationship between flyrock distance and its aforementioned influencing factors. According to the existing studies, flyrock estimation strategies can be grouped into three categories, i.e., mechanistic modelling, empirical approach and machine learning approach.

The mechanistic modelling compute the flyrock distance by fully identifying the physical mechanism behind blasting operation [16–18]. However, the required parameters like launch angle and launch velocity are hard to be collected. Furthermore, the developed mechanistic models are region dependent. In the empirical approach, an empirical equation is

* Corresponding author. School of Civil and Environmental Engineering, Queensland University of Technology, Gardens Point, QLD, 4000, Australia.
E-mail address: yilin.gui@qut.edu.au (Y. Gui).

https://doi.org/10.1016/j.ghm.2024.01.002
Received 14 October 2023; Received in revised form 9 January 2024; Accepted 15 January 2024
Available online 23 January 2024

fitted based on the assumption that the flyrock distance and influencing factors follow a certain relationship [19,20]. For example, a linear equation is fitted in Ref. [21] using burden, spacing and specific charge as variables. Similar to mechanistic models, the drawback of empirical equations is also site dependency, since the fitting of equation is only conducted for data ranges recorded at a specific location.

In recent years, with the development of artificial intelligence, machine learning techniques are frequently used in many fields of study for its strong learning ability as well as the ability to effectively relate input and output variables [22–26]. In the field of flyrock prediction, many machine learning models can be applied, including Artificial Neural Network (ANN), Adaptive Neuro Fuzzy Inference System (ANFIS), Support Vector Machine (SVM) and decision trees. ANN is probably the most famous and is widely used by the researchers to estimate blast induced flyrock distance. There are many types of ANN, i.e., Multilayer Perceptron (MLP), Recurrent Neural Network (RNN) and Convolutional Neural Network (CNN). Considering the characteristics of objective problem, most of the existing studies applied the MLP type of ANN in this field of study [27–33]. Since the ANN suffers from the problem of local minima, many existing studies developed hybrid learning ANN to address this issue, in which the meta-heuristic algorithms were combined with traditional back-propagation algorithm for model parameters optimization purpose. Relative studies in hybrid ANN models can be found in Refs. [34–37], where the Harris Hawks Optimization (HHO), Imperialist Competitive Algorithm (ICA), Genetic Algorithm (GA) and adaptive dynamical harmony search algorithm were used respectively. Additionally, the effectiveness of three different meta-heuristics in optimizing ANN were compared in Ref. [38], including ICA, GA and Particle Swarm Optimization (PSO). Although the use of meta-heuristic can guarantee for higher accuracy, the time efficiency of which is low due to the iterative training process. To improve the training efficiency, the Extreme Learning Machine (ELM) was used and combined with Biogeography-based Optimization (BBO) in Ref. [39]. Compared with traditional gradient based ANN, the ELM is able to train the model in one try and therefore reduce the training time of hybrid learning approach. Other than ANN, the applicability of ANFIS in estimating flyrock was evaluated in the studies [3,40]. The ANFIS can also be regarded as a variant of ANN, since it is the combination of Fuzzy Inference System (FIS) and ANN. Both ANN and ANFIS are parametric machine learning techniques. Beyond that, non-parametric models like decision tree models and SVM were also implemented by existing studies. The traditional Classification and Regression Tree (CART) was used by Hasanipanah to predict blast induced flyrock in Ulu Tiram quarry [41]. Ensemble learning methods like boosting and bagging can be applied to decision trees, and the ensemble tree models like Random Forest (RF), Gradient Boosted Decision Tree (GBDT) and extreme gradient boosting (XGBoost) are frequently applied for flyrock prediction by the existing studies [42–44]. The SVM is a kernel based algorithm, which is also frequently used to estimate blast induced flyrock distance [20,45]. Different from ANN of ANFIS, the model performances of these non-parametric models are affected by hyperparameters. Similarly, one can also apply the meta-heuristics for hyperparameters tuning to optimize the model performances. Examples of these can be found in the studies [46,47], where the Whale Optimization Algorithm (WOA) and HHO with multi-strategies (MSHHO) were used to optimize the hyperparameters of SVM respectively.

As mentioned previously, most of the existing studies attempted to obtain better performance of SVM by optimizing its hyperparameters via meta-heuristic approach. One of the tunable hyperparameters of SVM is the kernel parameter. However, rather than searching for an optimal kernel, the authors believe that an optimal kernel function can be generated using the combination of different kernels. Hence, the current study applied a multiple kernel learning method to develop a composite kernel function which is a linear combination of various kernels. This also reduce the number of parameters need to be tuned. Furthermore, considering the importance level of different contributing factors, a stacked structure is used to address this issue in order to further improve the model performance. The proposed method is further compared with 6 other machine learning models to verify its reliability, i.e., SVM, MK-SVM, LTSVM, ANN, RF and M5 Tree.

This paper is organized as follows. Section 2 describes the theory concept of the proposed method as well as the used blasting dataset. In Section 3, the details of development of all the aforementioned machine learning models are presented. The results obtained are subsequently reported in Section 4 along with a corresponding discussion on the model performances. Based on the discussion, a conclusion is drawn in the last section highlighting the contribution achieved by this study as well as the future scope.

2. Materials and method

2.1. Data collection

The data used in this study is collected from Sungun Copper Mine site, which is one of the largest porphyry copper mines in Iran. It is located in the East Azarbaijan province, at 46′43°E longitude and 38′42°N latitude, and is 2000 m above sea level. Copper is the main product of this mine, which can be extracted from its primary minerals, i.e., chalcopyrite, pyrite, chalcocite, cuprite and malachite. In addition to copper, gold, silver, and molybdenite can also be extracted from this mine. Table 1 provides a summary of the geological and geometrical features of this mine, and the map of the study area is presented in Fig. 1.

In Sungun Copper Mine, bench blasting with one free face is used for mineral extraction process. Main explosive material used was ANFO, and the blastholes were stemmed with drill-cutting particles. Detonating cord was used as initiation of blasting operations. The main blasting pattern was triangular, and the burden to spacing ratio was designed according to the characteristics of the blasting block in different areas of the mine. The blasting operations used a flat face method as blasting sequence, where the inter-hole delay time is set as zero and a delay happens between blasting rows. Flyrock is considered as one of the main ill effects of the blasting operations in this mine. As a result, this study attempted to develop a model predicting flyrock distance. For this purpose, 234 blasting events were designed and recorded, where 6 blasting parameters were collected, i.e., hole length, spacing, burden, stemming, powder factor, and specific drilling. The basic descriptive statistics of these features as well as the measured flyrock distance were summarized in Table 2. Fig. 2 illustrated the correlation matrix plot of the dataset, which can be used to study the level of relationship between target (flyrock) and its 6 influencing parameters.

According to the correlation coefficients demonstrated in Fig. 2, other than powder factor and specific drilling, the other features have an inverse relationship with flyrock. Furthermore, it can be observed that powder factor shows the biggest influence on flyrock. Compared with other features, specific drilling has the lowest correlation to flyrock, whose correlation coefficient is 0.1009, indicating a less significance.

Table 1
Geological and geometrical features of Sungun Copper Mine [44].

Geological/Geometrical Properties	Value
Geological reserve of the deposit	796 MT
Proved reserve	410 MT
Average grade	0.67%
Height of the working benches	12.5 m
Slope of the working benches	68′
Angle of the overall pit slope	37′
Width of the ramp	30 m
Slope of the ramp	5′
Age of the mine	Around 32 yr
Overall stripping ratio	1.7

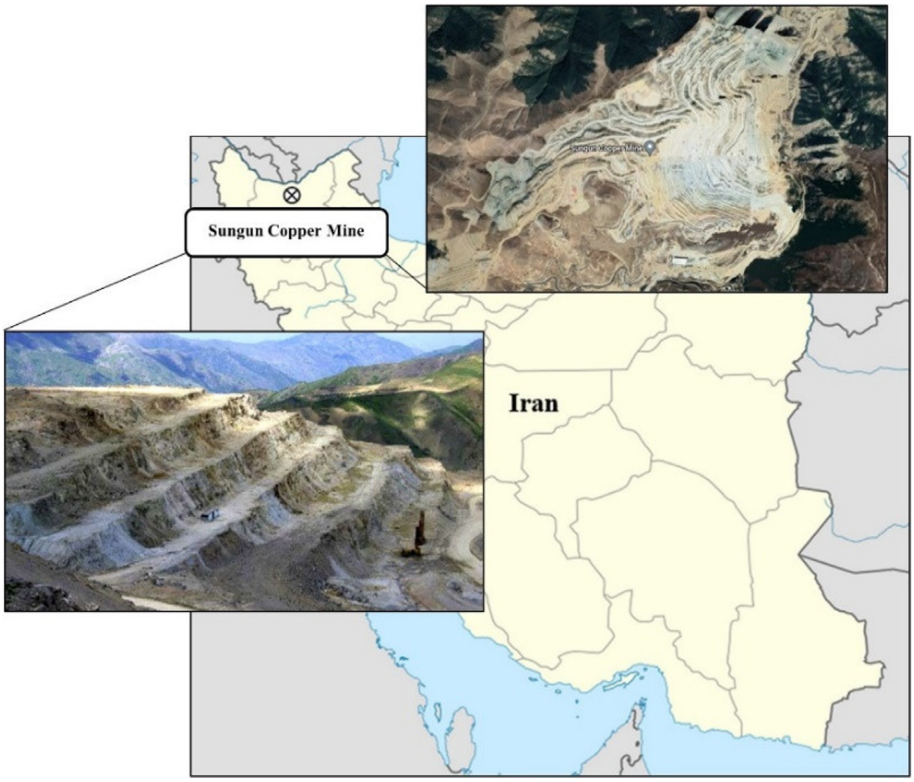

Fig. 1. Map of sungun copper mine site [44].

Table 2
Description of dataset.

	Unit	Min	Max	Mean	Standard deviation
Hole length	m	10	14	12.3098	1.1837
Spacing	m	2	6.5	4.5278	0.9009
Burden	m	2	5	3.6944	0.8154
Stemming	m	1.8	4.5	3.6637	0.7640
Powder factor	kg/m^3	0.2	0.93	0.4608	0.1977
Specific drilling	m	0.04	0.29	0.0729	0.0396
Flyrock	m	10	100	68.6838	17.4155

2.2. *Support vector machine*

Support Vector Machine (SVM) is a powerful and robust machine learning technique proposed by Cortes and Vapnik in 1995 [48,49]. It was first introduced to solve classification problem, and can be further extended to deal with regression task. Given a set of training data $\{\boldsymbol{x}_i, y_i\}_i^n$, SVM approximates the desired output y_i by fitting the following nonlinear regression hyperplane:

$$f(x) = \boldsymbol{w}^{\mathrm{T}}\varphi(\boldsymbol{x}) + b \tag{1}$$

where $\boldsymbol{w}$ and b are the weights and bias. $\varphi(\bullet)$ is the prespecified nonlinear mapping function. The purpose of SVM is to find the hyperplane that maximizes the margin, in which the margin is defined as the Euclidean norm of the weights, $\|\boldsymbol{w}\|$. Therefore, the objective function of SVM can be written as:

$$\text{minimize}: \frac{1}{2}\|\boldsymbol{w}\|^2 + C\sum_{i=1}^{n}|y_i - f(x_i)|_\varepsilon \tag{2}$$

where $|y_i - f(x_i)|_\varepsilon$ represents the ε-insensitive loss function, which has a tolerance of error within ε, defined as:

$$|y_i - f(x_i)|_\varepsilon = \begin{cases} 0, |y_i - f(x_i)| \leq \varepsilon \\ |y_i - f(x_i)| - \varepsilon, |y_i - f(x_i)| > \varepsilon \end{cases} \tag{3}$$

The positive constant C in equation (2) is a penalty coefficient that controls the degree to which the model can tolerate those datapoints that fall outside the ε-insensitive tube. Introducing two slack variables $\xi_i{}^+$ and $\xi_i{}^-$, equation (2) can be rewritten as:

$$\text{minimize}: \frac{1}{2}\|\boldsymbol{w}\|^2 + C\sum_{i=1}^{n}(\xi_i{}^+ + \xi_i{}^-) \tag{4}$$

$$\text{subject to}: \begin{array}{c} \forall i: y_i - f(x_i) \leq \varepsilon + \xi_i{}^+ \\ \forall i: f(x_i) - y_i \leq \varepsilon + \xi_i{}^- \\ \forall i: \xi_i{}^+, \xi_i{}^- \geq 0 \end{array} \tag{5}$$

To solve the above optimization problem, one can introduce non-negative Lagrange multipliers α_i^+, α_i^-, η_i^+ and η_i^- to the constraint (5) and reformulate equation (4) as:

$$\begin{aligned} L := & \frac{1}{2}\|\boldsymbol{w}\|^2 + C\sum_{i=1}^{n}(\xi_i{}^+ + \xi_i{}^-) - \sum_{i=1}^{n}(\eta_i^+\xi_i{}^+ + \eta_i^-\xi_i{}^-) \\ & - \sum_{i=1}^{n}\alpha_i^+(\varepsilon + \xi_i{}^+ - y_i + f(x_i)) - \sum_{i=1}^{n}\alpha_i^-(\varepsilon + \xi_i{}^- + y_i - f(x_i)) \end{aligned} \tag{6}$$

Taking the partial derivatives of equation (6) with respect to the primal variables (w, b, $\xi_i{}^+$, $\xi_i{}^-$) and setting them to zero, the following optimality can be obtained:

$$\frac{\partial L}{\partial b} = \sum_{i=1}^{n}(\alpha_i^+ - \alpha_i^-) = 0 \tag{7}$$

$$\frac{\partial L}{\partial \boldsymbol{w}} = \boldsymbol{w} - \sum_{i=1}^{n}(\alpha_i^+ - \alpha_i^-)\varphi(\boldsymbol{x}_i) = 0 \tag{8}$$

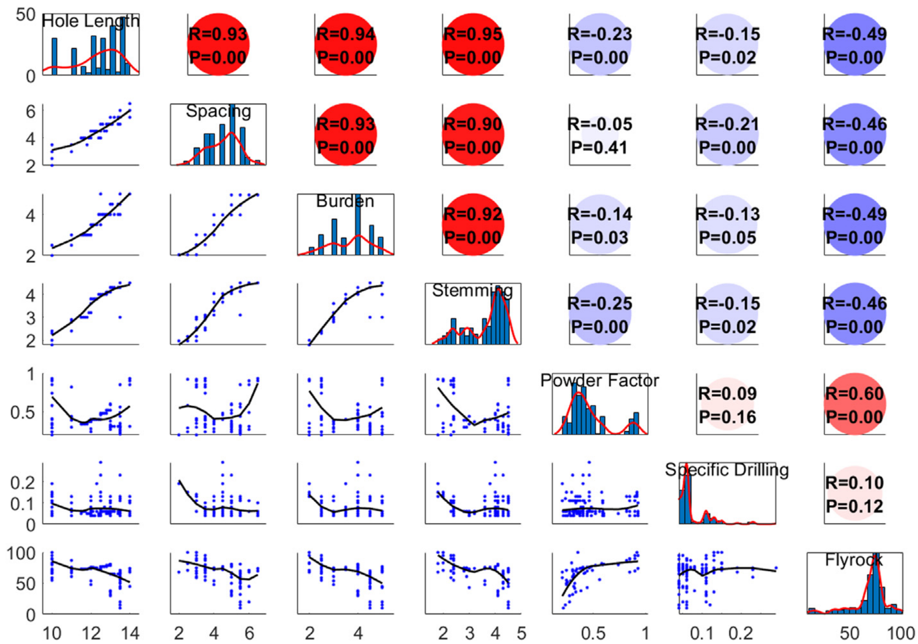

Fig. 2. Correlation Matrix of Dataset (histogram in diagonal line, correlation coefficients in upper triangular, and scatter plots in the lower triangular).

$$\frac{\partial L}{\partial \xi_i^{+,-}} = C - \alpha_i^{+,-} - \eta_i^{+,-} = 0 \tag{9}$$

Substituting equations (7)–(9) into equation (6), the η_i^+ and η_i^- can be eliminated and the dual optimization problem of SVM can be obtained as:

$$L := \frac{1}{2}\sum_{i=1}^{n}\sum_{j=1}^{n}(\alpha_i^+ - \alpha_i^-)\left(\alpha_j^+ - \alpha_j^-\right)K(\boldsymbol{x}_i, \boldsymbol{x}_j) + \varepsilon\sum_{i=1}^{n}(\alpha_i^+ + \alpha_i^-) - \sum_{i=1}^{n} y_i(\alpha_i^+ - \alpha_i^-) \tag{10}$$

$$\text{Subject to}: \begin{array}{l} \sum_{i=1}^{n}(\alpha_i^+ - \alpha_i^-) = 0 \\ \forall i, 0 \le \alpha_i^+, \alpha_i^- \le C \end{array} \tag{11}$$

The above constraint dual optimization problem can be solved using Sequential Minimal Optimization (SMO) algorithm. More details of SMO can be found in Refs. [50,51]. According to equation (8), the weight vector $\boldsymbol{w}$ in equation (1) can be replaced by $\sum_{i=1}^{n}(\alpha_i^+ - \alpha_i^-)\varphi(x_i)$, and therefore equation (1) can be reformulated as:

$$f(x) = \sum_{i=1}^{n}(\alpha_i^+ - \alpha_i^-)K(\boldsymbol{x}_i, \boldsymbol{x}) + b \tag{12}$$

The $K(a, b)$ in equations (10) and (12) denotes the kernel function representing the inner product $(\varphi(a), \varphi(b))$. Various kernel functions can be used, i.e., linear, polynomial and Gaussian kernel. They are defined as:

$$K(x_i, x_j) = x_i^{\mathrm{T}} x_j \tag{13}$$

$$K(x_i, x_j) = \left(x_i^{\mathrm{T}} x_j + 1\right)^d \tag{14}$$

$$K(x_i, x_j) = \exp\left(-\sigma\|x_i - x_j\|^2\right) \tag{15}$$

In equations (14) and (15), the coefficients d and σ represent the polynomial order and kernel length, respectively. In this study, the proposed model uses the multiple kernel learning method to construct a composite kernel function which is the linear combination of all these three kernel functions.

2.3. Multi-kernel SVM

According to the existing studies, the kernel function is highly correlated to the final fitting performance of SVM. Therefore, careful selection of kernel function and fine tuning of its parameters, i.e., polynomial order and kernel length, are necessary for SVM development. However, such process would be very time consuming. Hence, to reduce the effort devoted in finding an optimal kernel, this study uses a chunking based Multiple Kernel Learning (MKL) algorithm to replace the single kernel function by a linear combination of various kernels. The details of the proposed MKL method will be described in following.

1) *MKL Training:* As mentioned above, the kernel function $K(\bullet, \bullet)$ in the MK-SVM is represented by a linear combination of different single kernel functions and the kernel function can be expressed as:

$$\begin{array}{l} K_{\text{all}}(\bullet, \bullet) = \sum_{m=1}^{M}\beta_m K_m(\bullet, \bullet) \\ \text{s.t} \sum_{m=1}^{M}{\beta_m}^2 = 1, \beta_m \ge 0 \end{array} \tag{16}$$

where β_m is the combination coefficient. In equation (16), an l_2-norm constraint was imposed to ensure the non-sparsity of kernel mixture. Denote the term $(\alpha_i^+ - \alpha_i^-)$ in equation (12) as α_i, the combination coefficient β_m can be calculated according to Ref. [52]:

$$\beta_m = \frac{\left({\beta_m}^2 \boldsymbol{\alpha}^T \boldsymbol{K}_i \boldsymbol{\alpha}\right)^{1/3}}{\left(\sum_{m=1}^{K}\left({\beta_m}^2 \boldsymbol{\alpha}^T \boldsymbol{K}_m \boldsymbol{\alpha}\right)^{2/3}\right)^{1/2}} \tag{17}$$

where $\boldsymbol{\alpha}$ is the column vector of α_i. In the MKL method, the combination coefficient β and the weight vector of SVM were updated iteratively until the normalized maximal constraint violation of MKL converge to the predetermined precision. The termination criteria can be formulated as:

$$\left|1 - \frac{G}{G_{\text{old}}}\right| \le \epsilon \tag{18}$$

where ϵ is a very small positive precision value and G is the objective function of MKL, written as:

$$G = \sum_i y_i \alpha_i - \frac{1}{2}\sum_{m=1}^{K} \beta_m \boldsymbol{\alpha}^T \boldsymbol{K}_m \boldsymbol{\alpha} \tag{19}$$

2) *Kernel Generation:* All the three kinds of kernel function presented in equation (13)–(15) are included in the composite kernel. As for the kernel parameters, various of polynomial functions and Gaussian functions are constructed using different values of d and σ. 13 different values of σ were used, $[0.1, 0.5, 1, 1.5, 2, 3, 4, 5, \ldots, 10]$, and the polynomial order varies from 1 to 3. Beyond that, since the training input always consists of various attributes, kernel functions using single attributes are also constructed to further increase the diversity of kernels in order to enable more information can be included. Assume the dimensionality of training input $\boldsymbol{x}$ is $\boldsymbol{N}$, then the kernel functions are generated using (N+1) features presented as following:

$$\begin{cases} [x_i]_{i=1,2,\ldots,N} \\ [x_1, x_2, \ldots, x_N] \end{cases} \tag{20}$$

Therefore, for example, if the input vector is 4-dimensional, 80 kernel functions ((13 + 3)*5) will be generated.

Based on the above description, the pseudo code for MK-SVM training is presented as following.

Algorithm 1. MK-SVM Training

Input: Training data: $\{\boldsymbol{x}_i, y_i\}$, predefined precision: ϵ
Output: $\boldsymbol{\alpha}$ and $\boldsymbol{\beta}$
[1]Construct kernel matrices $\{\boldsymbol{K}_m\}_{m=1,2,\ldots,M}$ based on Eq. (20)
[2]Initialize $\beta_m = \sqrt{\frac{1}{M}}$
[3] $q=0$
Repeat
[4]Update $\boldsymbol{\alpha}(q)$ using SMO
[5]Update $\boldsymbol{\beta}(q)$ using Eq. (17)
[6] $q=q+1$
Until $\left\lvert 1 - \frac{G(q)}{G(q-1)} \right\rvert \le \epsilon$
Return $\boldsymbol{\alpha}$ and $\boldsymbol{\beta}$

In algorithm 1, the training of SVM ($\boldsymbol{\alpha}$ calculation) used the SMO algorithm, the details of which can be found in Ref. [51].

2.4. Stacked structure

The stacking method is an ensemble learning method, which uses the integration of several base learners to form a meta-learner to improve the predictive capability. In a stacked model, the base learners are trained in the first place, and the meta learner is subsequently developed using the outputs of the base learners as training inputs. In the proposed stacked MK-SVM model, all the base learners and the meta-learners used the MK-SVM introduced in the previous section for modelling purpose. The development of the proposed stacked MK-SVM was illustrated in Fig. 3.

The proposed stacked model consists of only one base learner, which is trained using the specific drilling as model input. This is because its impact on the flyrock distance is less significant compared to the other parameters based on the previous correlation analysis. According to Fig. 2, the correlation coefficients between other parameters and flyrock are larger than 0.4, whereas that for specific drilling is only 0.12, which indicates a less significance. Based on the findings of existing studies [53, 54], directly using those less correlated features with other influencing factors together as input might worsen the model performance. Inspired by the stacking method, the authors add a base learner to address this issue by studying the latent relationship between specific drilling and flyrock distance, and the generated feature is then fused with other feature in the meta-learner level to form the final predictor. Such stacked structure is able to improve the correlation level of the less significant features via the base learner. Hence, in the meta-learner level, all the input attributes have relatively high relationship with desired output, and the model accuracy can be improved. Furthermore, it needs to be mentioned that the kernel generation strategy described in equation (20) is not applicable for the base MK-SVM development, since it is trained using one attribute and only the kernel functions with different length and order will be generated. Subsequently, all the attributes of training data along with the outputs of all base learners will be used as input to train the meta learner. The training of meta-learner follows all the details described in the previous section.

3. Model development

3.1. Model evaluation

In this study, the performances of the models are evaluated by three evaluation indices, Root Mean Squared Error (RMSE), Mean Absolute Error (MAE) and Variance Accounted For (VAF). The formulas used to calculate these indices are given as follows:

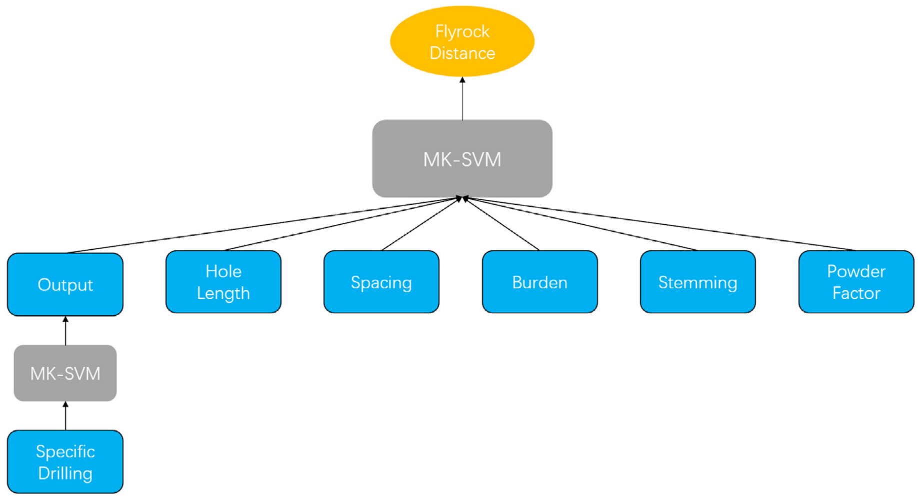

Fig. 3. Structure of stacked MK-SVM

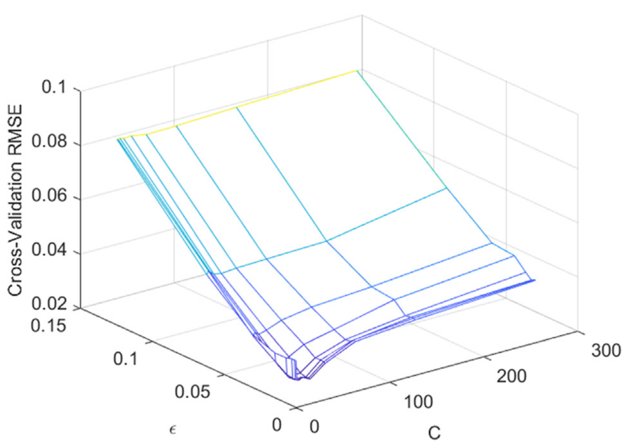

Fig. 4. Cross-validation process of stacked MK-SVM

$$\mathrm{RMSE} = \sqrt{\frac{\sum_{1}^{n}\left(\tilde{y}_i - y_i\right)^2}{n}} \tag{21}$$

$$\mathrm{MAE} = \frac{\sum_{i=1}^{n}\left|\tilde{y}_i - y_i\right|}{n} \tag{22}$$

$$\mathrm{VAF} = \frac{1 - \mathrm{var}(y_i - \tilde{y}_i)}{\mathrm{var}(y_i)} \times 100 \tag{23}$$

where $\tilde{y}_i$ represents predicted, y_i is the observed value and $\overline{y}$ denotes the mean value.

3.2. Model development

In this section, the development process of the proposed stacked MK-SVM model was described. For comparison purpose, several existing machine learning models were also implemented, including three SVM models, i.e., MK-SVM (without stacking), traditional SVM, and Lagrangian Twin SVM (LTSVM). The LTSVM is a state of art SVM variant model proposed in Ref. [55], the innovation of which will be introduced in the following section. Other than SVM and its variants, some widely used machine learning models such as ANN, RF, M5 Tree were also developed and compared. For evaluation purpose, 34 sets of blasting dataset were randomly selected out of the whole dataset and served as the testing dataset. The remaining 200 sets of data were used as training dataset. To obtain the optimum model performances, a 5-fold cross validation process was used to determine the optimal hyperparameters, where each fold of validation dataset consists of 20 sets of randomly selected training data. Different hyperparameter combinations were generated using grid search method, and the mean cross validation RMSE was used as the standard to select the optimal sets of hyperparameters. The models were subsequently trained again on the whole training dataset after the optimal hyperparameters were obtained. The details of the hyperparameters tuning process were illustrated as following and the obtained hyperparameters for models were summarized in Table 3.

Table 3
Optimal hyperparameters of models.

	Hyperparameters
Stacked MK-SVM	$C = 16, \varepsilon = 2^{-8}$
MK-SVM	$C = 4, \varepsilon = 2^{-7}$
SVM	$C = 32, \varepsilon = 2^{-6}, \sigma = 0.5$
LTSVM	$C_1 = C_2 = 32, \varepsilon_1 = \varepsilon_2 = 2^{-10}, \sigma = 10$
ANN	$[6-2-10-1]$
RF	$ntree = 300, mtry = 0.4$
M5 Tree	$depth = 4, minleafsize = 10$

1) *MK-SVM and Stacked MK-SVM:* Since the proposed multiple kernel learning approach uses a composite kernel function, the tuning of kernel parameters for the stacked MK-SVM and MK-SVM was not necessary. Hence, only the regularization coefficient C and half width of ε-insensitive band ε were tuned. 9 different values of C were used to search for the optimal, $\{2^0, 2^1, 2^2, \ldots, 2^8\}$. As for ε, it should be a very small positive constant, and therefore was searched in $\{2^{-10}, 2^{-9}, 2^{-8}, \ldots, 2^{-3}\}$. The stack MK-SVM involves two separate MK-SVM learners, and the same C and ε values were applied, that is $C_{\text{base}} = C_{\text{meta}}$ and $\varepsilon_{\text{base}} = \varepsilon_{\text{meta}}$. For illustration purpose, the cross-validation result of stacked MK-SVM was presented in Fig. 4. The cross-validation process reported an optimal combination of $\{C, \varepsilon\}$ for stacked MK-SVM was $\{16, 2^{-8}\}$, and the MK-SVM with $\{C = 4, \varepsilon = 2^{-7}\}$ has the best validation performances.

2) *SVM and LTSVM:* The SVM developed here refers to the traditional SVM without multiple kernel learning. Therefore, other than C and ε, the kernel parameters of SVM need to be determined. All of the three types of kernel function were taken into consideration. Similar to the multiple kernel learning approach, 13 different kernel length (σ) values were used for Gaussian function, $[0.1, 0.5, 1, 1.5, 2, 3, 4, 5, \ldots, 10]$, and the order of polynomial function varied from 1 to 3. As for

LTSVM, its difference between traditional SVM is that it attempts to fit two regression hyperplanes whereas traditional SVM only have one. More details of TSVM can be found in Refs. [55,56]. Therefore, the number of tunable hyperparameters of TSVM is doubled. For LTSVM, two regularization coefficients C_1 and C_2, two ε values, ε_1 and ε_2 need to be determined. For simplicity, the authors followed the experiment process presented in Refs. [55,56] and applied the same hyperparameters for both hyperplanes, that is, $C_1 = C_2$ and $\varepsilon_1 = \varepsilon_2$. The searching space of C, ε and kernel parameters was the same as aforementioned. According to the validation results, the optimal combinations of $\{C, \varepsilon\}$ were $\{32, 2^{-6}\}$ and $\{32, 2^{-10}\}$ for SVM and LTSVM respectively, and the optimal kernel for both of them was Gaussian function, with kernel length of 0.5 and 10 respectively.

3) *ANN:* The ANN developed in this study is a traditional MLP trained by the Levenberg-Marquardt algorithm. To obtain an optimal ANN, various network structures were designed. Considering the size of dataset, deep networks were avoided to reduce the risk of overfitting. In this study, the maximum number of hidden layers was set as 2, and the number of hidden neurons was determined in the range $\{2, 4, 6, 8, \ldots, 20\}$. The optimal network topology obtained by the cross-validation process was $[6 - 2 - 10 - 1]$.
4) *RF:* The RF is an ensemble learning algorithm which uses the concept of bagging to build a collection of Classification and Regression Tree (CART). In RF, each CART is trained individually using a subset generated by bootstrap sampling method, and the overall output is determined as the averaged output of all trees. Additionally, to further increase the diversity between CARTs, an attribute selection process is used in which a predefined number of attributes are randomly selected and used to search for the best split at each node. Therefore, the tunable hyperparameters of RF are the number of trees (ntree) and the number of attributes selected (mtry). In this study, the searching space of these two hyperparameters were $\{10, 50, 100, 200, 300, \ldots, 1000\}$ and $\{2, 3, \ldots, 6\}$. Following the aforementioned hyperparameters tuning process, the RF with $\mathrm{ntree} = 300$ and $\mathrm{mtry} = 0.4$ obtained the best cross validation performance.
5) *M5 Tree:* The M5 Tree is a model tree algorithm. Different from GBDT, the M5 Tree is a single decision tree. It searches for the best split at each node by selecting the attribute that has the maximal reduction in output variance. Beyond that, it also fits a linear equation rather than a single value to approximate the target at each node. Hyper-parameters like maximum tree depth (depth) and minimum leaf size ($\mathrm{minleafsize}$) were tuned to obtain an optimal M5 Tree. Considering the size of dataset, the searching space of these two hyperparameters was determined as $[2, 3, 4, \ldots, 20]$ and $[5, 10, 20, 30, \ldots, 100]$. The optimal hyperparameters of M5 Tree obtained by the cross-validation process were $\mathrm{depth} = 4$ and $\mathrm{minleafsize} = 10$.

4. Results and discussion

4.1. Discussion of model performances

In the previous section, 7 machine learning models were developed, i.e., stacked MK-SVM, MK-SVM, SVM, LTSVM, ANN, RF and M5 Tree. For evaluation purpose, the performances of these models were compared on the testing dataset using the three evaluation indices presented in the previous section. The obtained results at both training and testing datasets were summarized in Table 4, and a corresponding stacked graph was shown in Fig. 5 depicting the overall score of each model. For illustration of fitting performance, the predicted versus measured flyrock distance value at training and testing stage were presented in Figs. 6 and 7. A Taylor graph was given in Fig. 8 to further compare the performance differences between models at testing stage.

According to the results presented in Table 4, the proposed stacked MK-SVM achieved the best overall performances. Notably, at both training and testing stages, the proposed method obtained the highest score on every evaluation criterion, with the lowest RMSE and MAE of 1.73/1.74 and 0.58/1.08, as well as the highest VAF value of 98.95/99.25, providing ample evidence on the superiority of the proposed method.

Based on the stacked graph presented in Fig. 5, other than the proposed method, the performances of SVM and its variant models, i.e., MK-SVM and LTSVM, were better than the other machine learning models. This indicates that SVM models were more capable for flyrock prediction. Among the remaining models, the reliability of M5 Tree was the lowest. This was evidenced by the plot of prediction results presented in Figs. 6 and 7, where the predictions of M5 Tree were less correlated to the ground truth value. The ANN and RF achieved similar training accuracy, as their obtained training evaluation indices were close. However, at testing stage, the difference between them was obvious. RF significantly underperformed ANN at two evaluation criterions, i.e., RMSE and VAF, which were 4.96/6.27 and 94.10/90.50, which indicates a less collinearity with the desired output. This can also be observed from the Taylor diagram given in Fig. 8 where there is a significant gap between the representations of these two models. Hence, compared with RF, ANN demonstrated stronger reliability.

Taking a deeper look into the performances between the three types of compared SVM-based models, i.e., SVM, MK-SVM and LTSVM, the MK-SVM model achieved higher overall score than the other two models according to the stacked graph presented in Fig. 5. This is because MK-SVM slightly outperformed them at every evaluation criterion at both training and testing stages. However, the performance gap between them is not huge. Based on the Taylor diagram presented in Fig. 8, their

Table 4
Training and testing performances of models.

	Training Performance						
	RMSE	Score	MAE	Score	VAF	Score	Rank
Stacked MK-SVM	1.73	7	0.58	7	98.95	7	1
MK-SVM	1.99	6	0.92	6	98.61	6	2
SVM	2.70	4	1.52	4	97.44	4	4
LTSVM	2.07	5	1.11	5	98.48	5	3
ANN	4.30	3	3.05	2	93.48	3	5
RF	4.60	2	2.57	3	92.53	2	6
M5 Tree	6.75	1	4.04	1	83.94	1	7
Stacked MK-SVM	1.74	7	1.08	7	99.25	7	1
MK-SVM	4.58	6	2.87	6	94.79	6	2
SVM	4.74	4	3.21	5	94.43	5	3
LTSVM	4.72	5	3.42	4	94.39	4	4
ANN	4.96	3	3.53	3	94.10	3	5
RF	6.27	2	3.82	2	90.50	2	6
M5 Tree	7.44	1	4.72	1	86.37	1	7

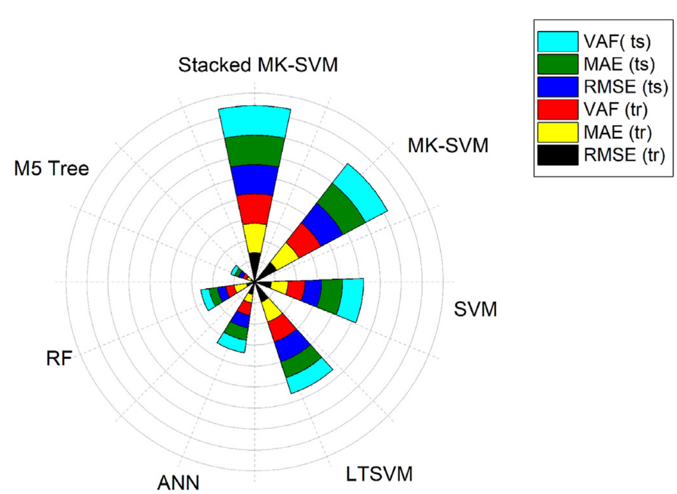

Fig. 5. Comprehensive stacked graph of models.

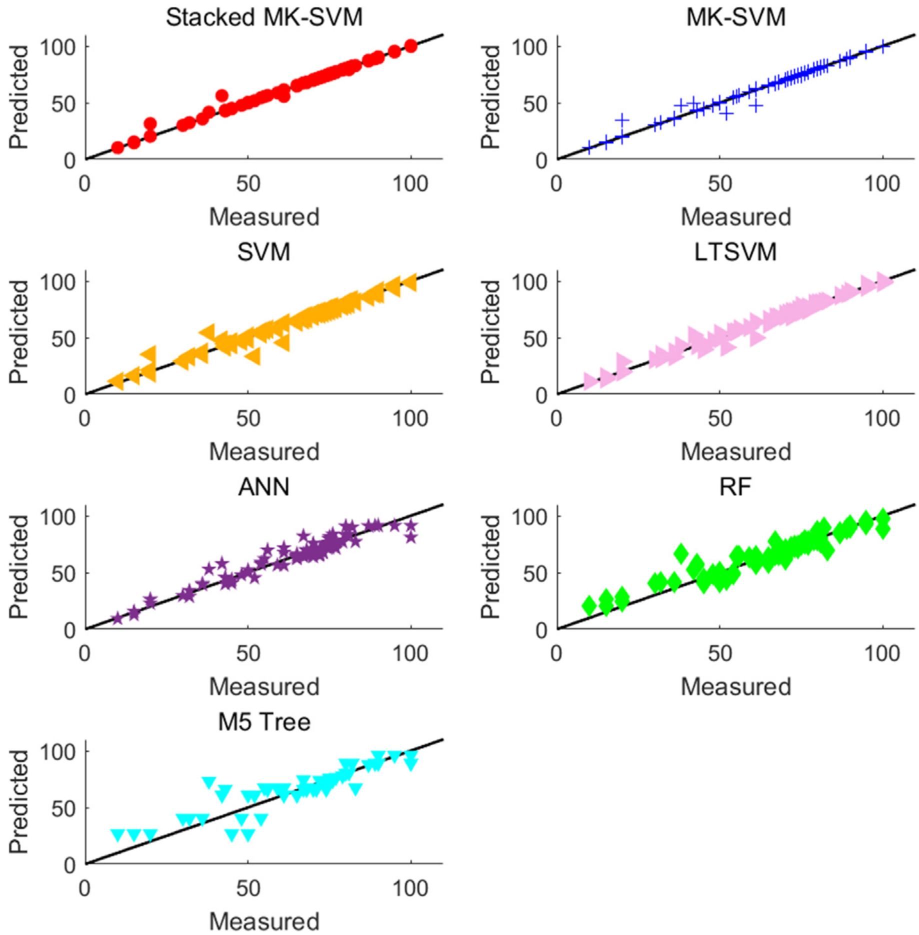

Fig. 6. Training results of models.

accuracy on testing dataset was very close, as their representation points located closely, indicating similar correlation level and RMSE value. Among them, the LTSVM achieved closer standard deviation value to the desired output. The obtained RMSE and correlation coefficient values of MK-SVM were slightly better. The testing results given in Table 4 also support such statement, since their obtained evaluation indices values were very close. Hence, it is hard to tell which one performs better among them. However, compared with these three models, the progress made by proposed model was huge. The authors consider the reason behind this is due to the use of specific drilling as model input. As aforementioned, the specific drilling was less correlated to the flyrock distance, and using it directly as model input could worsen the model performance. To investigate the reliability of this hypothesis, the aforementioned three SVM models were redeveloped in which the specific drilling was removed from model input. For simplicity, all the hyperparameters were set as the same given in Table 3. The obtained results were presented in Table 5.

In Table 5, the terms 'tr' and 'ts' represent training and testing stages, respectively, and the sign '*' denotes the redeveloped models. According to the results presented in Tables 5 and it is obvious that removing the specific drilling from model input can greatly enhance the testing performance. Meanwhile, the training performances of these models can still remain as previously, where only slight difference could be seen. Therefore, this provides ample evidence on the reliability of the aforementioned statement. Although the reliability of these models was improved by neglecting the impact of specific drilling, the performance of the proposed method was still significant, which once again demonstrates the superiority of the proposed method. This implies that simply removing the specific drilling from the model input is not the best option, since it is also affecting the blasting operation. Therefore, the impact of specific drilling on the distance of induced flyrock phenomenon can be learned by the first MK-SVM in the stacking structure. Subsequently, incorporating the learned feature into the input of the second MK-SVM with other features is able to explore in-depth the relationship between blast induced flyrock and all the influencing factors given. As a result, the proposed model is able to improve the model accuracy with the increase of input factors.

Apart from that, since the proposed model used a stacked structure and the training process of which is a two-step procedure. Hence, compared with MK-SVM, the computational complexity of the proposed method is increased, as the training process of MK-SVM needs to be repeated. Since the MK-SVM uses a multiple kernel learning approach, the time complexity of which is also larger than traditional SVM. As a result, to compare the time complexity, the running times of all the 7 developed models were summarized in Table 6.

As stated previously, it can be observed from Table 6 that the proposed method requires more training time compared with MK-SVM and traditional SVM. Moreover, the proposed method is faster than LTSVM and M5 Tree. Although the proposed stacked MK-SVM sacrifices the computational complexity to achieve higher accuracy, the running time was only 0.58s, which is acceptable.

Overall, all the developed models demonstrated good potential for estimating blast induced flyrock distance. Compared with other models, the proposed stacked MK-SVM is able to make use of all the given features, and hence achieves the highest accuracy.

4.2. Error analysis

Error analysis was implemented on the developed models to further

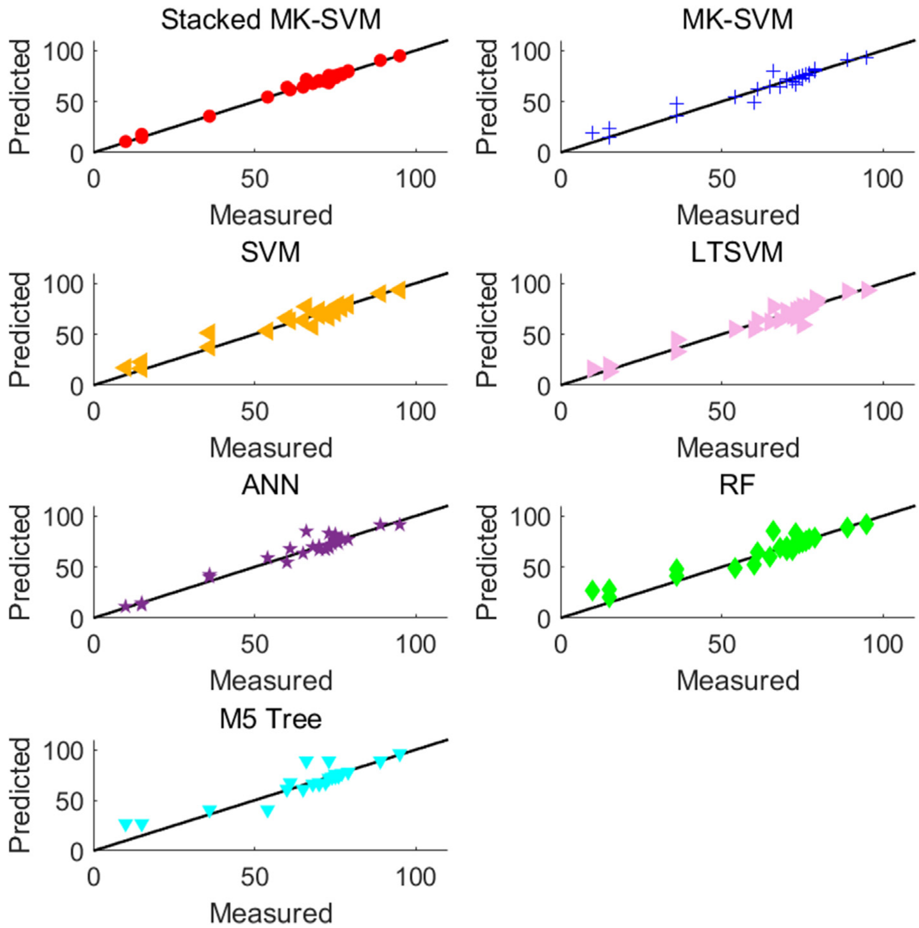

Fig. 7. Testing results of models.

measure the uncertainty of these models in estimating flyrock distance, in which the mean value of error $\bar{e}$ and standard deviation of error S_e are calculated according to the following equations:

$$\bar{e} = \frac{\sum_{i=1}^{n} e_i}{n} \tag{24}$$

$$S_e = \sqrt{\frac{\sum_{i=1}^{n} (e_i - \bar{e})^2}{n-1}} \tag{25}$$

The positivity or negativity of $\bar{e}$ indicates the overestimation or underestimation of the prediction model. The scatter of prediction error can be evaluated by S_e. Therefore, a high value of S_e implies a high uncertainty of model prediction. Accordingly, the 95 % error confidence band can be calculated by $\pm 1.96 S_e$. Beyond that, the Nash-Sutcliffe Efficiency (NSE) is also calculated to further evaluate the model performances. The calculation of NSE is based on the squared error between observation and model predictions:

$$NSE = 1 - \frac{\sum_{i=1}^{n} {e_i}^2}{\sum_{i=1}^{n} (t_i - \bar{t})^2} \tag{26}$$

where t_i represents the measured flyrock distance and $\bar{t}$ is the mean value of all measure flyrock distance. A NSE value of 1 means a perfect approximation. It is widely used measure the approximation performance of the prediction model [57–59]. Table 7 presents the analysis results, including the maximum error, mean error, uncertainty bandwidth and NSE.

According to the results presented in Table 7, only the LTSVM has an $\bar{e}$ value of -0.20, indicating an underestimation. All the other models tend to overestimate the flyrock distance and therefore the identified safety warning distance could be credible. Furthermore, among all the developed models, the stacked MK-SVM is considered as the most reliable one, as it has the minimum value of e_{max} (5.70), which is significantly smaller than the remaining models. Meanwhile, it also provides the lowest uncertainty bandwidth, which is $\pm$ 3.4104, and this implies that the predictions of the proposed model are more reliable. Moreover, the NSE value of the proposed method is 0.9924, which is significantly higher than the remaining models, indicating a strong fitting performance, whereas the predictions of M5 Tree were less correlated to the observed values with NSE value of 0.8604. Based on the error analysis result, the superiority of the proposed method was confirmed, as it demonstrated the strongest reliability and approximation performance.

5. Conclusion

In this study, an attempt has been made to predict the blast induced flyrock. For this purpose, 234 sets of data were collected from Sungun Copper Mine site, where 6 influencing factors were recorded, i.e., hole length, stemming, burden, spacing, powder factor and specific drilling. The correlation analysis process reported that the importance level of specific drilling was significantly lower than the other 5 features. Taking this issue into consideration, the authors proposed a special stacked MK-SVM model to make use of every feature. In the proposed stacked model, the base MK-SVM uses only the specific drilling as input, and the output of which is then incorporate with other 5 features and used as input of the meta learner. To evaluate the reliability of the proposed approach, 6

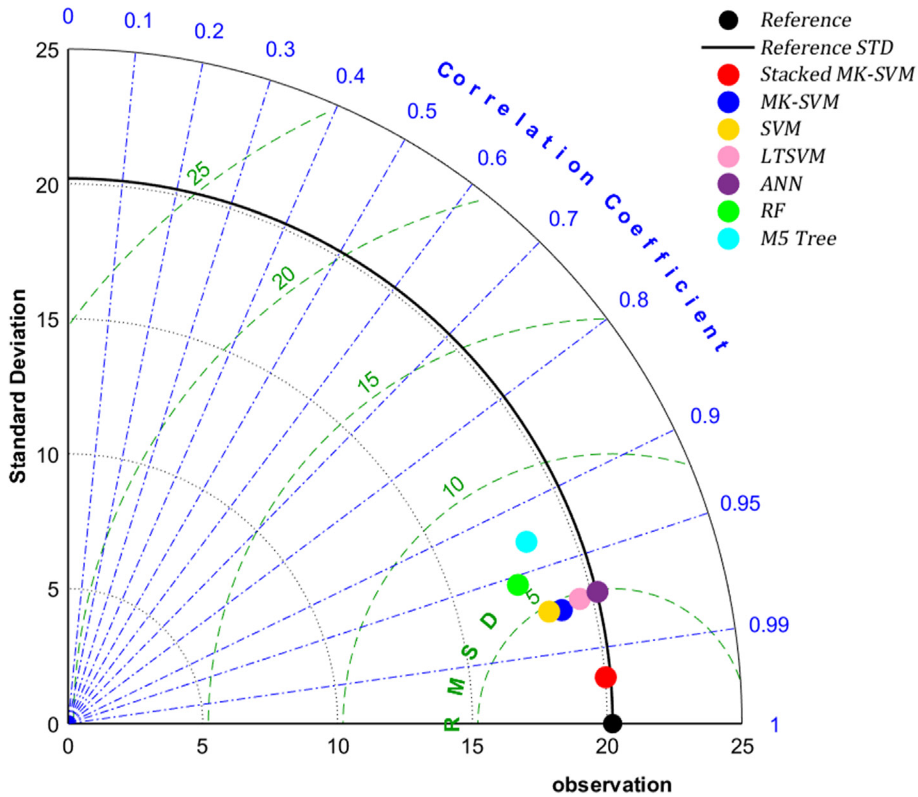

Fig. 8. Taylor plot of testing results.

Table 5
Comparison between SVM models with and without specific drilling.

	SVM	SVM*	MK-SVM	MK-SVM*	LTSVM	LTSVM*
RMSE (tr)	2.70	2.58	1.99	2.14	2.07	2.24
RMSE (ts)	4.74	2.83	4.58	3.00	4.72	3.59
MAE (tr)	1.52	1.67	0.92	1.02	1.11	1.29
MAE (ts)	3.21	2.06	2.87	2.14	3.42	2.43
VAF (tr)	97.44	98.00	98.61	98.40	98.48	98.95
VAF (ts)	94.43	97.67	94.79	97.76	94.39	96.77

Table 6
Running time of models.

	Running Time
Stacked MK-SVM	0.58 s
MK-SVM	0.22 s
SVM	0.07 s
LTSVM	1.04 s
ANN	0.26 s
RF	0.38 s
M5 Tree	0.91 s

Table 7
Uncertainty analysis of model performance.

	Max error (e_{max})	Average error ($\bar{e}$)	Uncertainty Bandwidth	NSE
Stacked MK-SVM	5.70	0.25	± 3.4104	0.9924
MK-SVM	13.50	0.58	± 9.0356	0.9470
SVM	15.40	0.60	± 9.3492	0.9434
LTSVM	− 15.83	− 0.20	± 9.3688	0.9438
ANN	18.89	1.11	± 9.6236	0.9379
RF	18.99	1.31	± 12.2108	0.9006
M5 Tree	22.90	1.14	± 14.6216	0.8604

other machine learning models were implemented as comparison, i.e., SVM, MK-SVM, LTSVM, ANN, RF and M5 Tree. For modelling and evaluation purpose, 34 sets of blasting data were randomly selected as testing dataset and the remaining data were used for model development. During the modelling procedure, the hyperparameters of these models were tuned using grid search method with a 5-fold cross validation process. Subsequently, the model performances were evaluated on the testing dataset using three evaluation criterions, RMSE, MAE and VAF.

Based on the evaluation results, the proposed stacked MK-SVM outperformed all the other models at both training and testing stage by achieving RMSE of 1.73/1.74, MAE of 0.59/1.08, and VAF of 98.95/99.25. It is therefore regarded as the most reliable model in predicting blast induced flyrock in Sungun Copper Mine site. The authors also found out that the SVM and its variants are more capable for flyrock prediction compared to ANN, RF and M5 Tree. Beyond that, the performance of these SVM models can be further improved if the specific drilling is removed from model input, and this supports the statement made in section 2.4 that the direct use of specific drilling can worsen the model performance. Rather than simply neglecting the impact of specific drilling, the proposed model is able to make use of it with the use of the proposed stacking structure, and hence achieve higher accuracy. All the comparison results have illustrated the superiority of the proposed model over the others.

Although the proposed stacked MK-SVM model demonstrated satisfactory prediction accuracy in the current study, there are still some drawbacks and limitations that need to be improved in the future. Firstly, the dataset used for model development and evaluation only consist of the blasting data collected from Sungun Copper Mine site and therefore whether the stacked structure is also applicable in other area is not examined. Furthermore, in the collected dataset, only the blasting parameters are available, whereas the uncontrollable parameters describing the variation of geological condition such as rock quality designation (RQD) are not included. Considering the above issue, the proposed model is well capable for predicting blast induced flyrock in

Sungun Copper Mine site, but the applicability of this prediction model in other sites is questionable. Therefore, the collection of blasting data from various sites and incorporate geological features as model input are the main objectives of future study, which enable us to further improve the model accuracy and evaluate the predictive capability of model on various site. Additionally, with the increased model inputs, modification on the stacked structure would be necessary.

Declaration of competing interest

All authors have no conflict of interest.

Acknowledgement

The first author (R. Zhang) would like to thank the financial support from Queensland University of Technology and the China Scholarship Council, on this study.

References

[1] K. Manoj, M. Monjezi, "Prediction of flyrock in open pit blasting operation using machine learning method,", Int. J. Min. Sci. Technol. 23 (2013) 313–316.
[2] T. Singh, V. Singh, "An intelligent approach to prediction and control ground vibration in mines,", Geotech. Geol. Eng. 23 (2005) 249–262.
[3] M. Rezaei, M. Monjezi, A.Y. Varjani, "Development of a fuzzy model to predict flyrock in surface mining,", Saf. Sci. 49 (2011) 298–305.
[4] M. Hajihassani, D.J. Armaghani, H. Sohaei, E.T. Mohamad, A. Marto, "Prediction of airblast-overpressure induced by blasting using a hybrid artificial neural network and particle swarm optimization,", Appl. Acoust. 80 (2014) 57–67.
[5] R. Zhang, Y. Li, Y. Gui, J. Zhou, "Prediction of blasting induced air-overpressure using a radial basis function network with an additional hidden layer,", Appl. Soft Comput. 127 (2022) 109343.
[6] Y. Gui, Z. Zhao, L. Jayasinghe, H. Zhou, A. Goh, M. Tao, Blast wave induced spatial variation of ground vibration considering field geological conditions, Int. J. Rock Mech. Min. Sci. 101 (2018) 63–68.
[7] B. Jayasinghe, Z. Zhao, A.T.C. Goh, H. Zhou, Y. Gui, "Attenuation of rock blasting induced ground vibration in rock-soil interface,", J. Rock Mech. Geotech. Eng. 11 (2019) 770–778.
[8] Y.L. Gui, Z.Y. Zhao, H.Y. Zhou, A.T.C. Goh, L.B. Jayasinghe, "Numerical simulation of rock blasting induced free field vibration,", Procedia Eng. 191 (2017/01/01/2017) 451–457.
[9] L.B. Jayasinghe, H. Zhou, A. Goh, Z. Zhao, Y. Gui, "Pile response subjected to rock blasting induced ground vibration near soil-rock interface,", Comput. Geotech. 82 (2017) 1–15.
[10] D. Ali, H. Abbas, T. Abdullah, "Numerical analysis of stress distribution during tunneling in clay stone rock,", Int. J. Eng. 33 (2020) 1472–1478.
[11] D. Li, M. Koopialipoor, D.J. Armaghani, "A combination of fuzzy Delphi method and ANN-based models to investigate factors of flyrock induced by mine blasting,", Nat. Resour. Res. 30 (2021) 1905–1924.
[12] R.S. Faradonbeh, D. Jahed Armaghani, M. Monjezi, "Development of a new model for predicting flyrock distance in quarry blasting: a genetic programming technique,", Bull. Eng. Geol. Environ. 75 (2016) 993–1006.
[13] E. Ghasemi, M. Sari, M. Ataei, "Development of an empirical model for predicting the effects of controllable blasting parameters on flyrock distance in surface mines,", Int. J. Rock Mech. Min. Sci. 52 (2012) 163–170.
[14] S. Bhandari, "Engineering Rock Blasting Operations,", 1997.
[15] T. Bajpayee, T. Rehak, G. Mowrey, D. Ingram, Blasting injuries in surface mining with emphasis on flyrock and blast area security, J. Saf. Res. 35 (2004) 47–57.
[16] T. Little, D. Blair, "Mechanistic Monte Carlo models for analysis of flyrock risk,", Rock fragmentation by blasting 9 (2010) 641–647.
[17] J. Roth, A Model for the Determination of Flyrock Range as a Function of Shot Conditions, NTIS, 1979.
[18] J. Workman, P. Calder, Flyrock prediction and control in surface mine blasting, International Society of Explosives Engineers, Cleveland, OH (United States), 1994.
[19] N. Lundborg, A. Persson, A. Ladegaard-Pedersen, R. Holmberg, "Keeping the lid on flyrock in open-pit blasting,", Eng. Min. J. 176 (1975) 95–100.
[20] H. Amini, R. Gholami, M. Monjezi, S.R. Torabi, J. Zadhesh, "Evaluation of flyrock phenomenon due to blasting operation by support vector machine,", Neural Comput. Appl. 21 (2012) 2077–2085.
[21] A. Aghajani-Bazzazi, M. Osanloo, Y. Azimi, "Flyrock prediction by multiple regression analysis in Esfordi phosphate mine of Iran,", in: Proceedings of the 9th International Symposium on Rock Fragmentation by Blasting, Granada, Spain, 2009, pp. 649–657.
[22] R. Zhang, Z. Cheng, Z. Zhang, Z. Chen, R. Ernst, M. Santosh, "Formation of tarim large igneous province and strengthened lithosphere revealed through machine learning,", J. Geophys. Res. Solid Earth 128 (2023) e2022JB025772.
[23] G. Zhang, N.S. Hamzehkolaei, H. Rashnoozadeh, S.S. Band, A. Mosavi, "Reliability assessment of compressive and splitting tensile strength prediction of roller compacted concrete pavement: introducing MARS-Goa-MCS,", Int. J. Pavement Eng. 23 (2022) 5030–5047.
[24] R. Zhang, C. Zhang, M. Yu, "A similar day based short term load forecasting method using wavelet transform and LSTM,", IEEJ Trans. Electr. Electron. Eng. 17 (2022) 506–513.
[25] J. Zhou, Y. Qiu, M. Khandelwal, S. Zhu, X. Zhang, "Developing a hybrid model of Jaya algorithm-based extreme gradient boosting machine to estimate blast-induced ground vibrations,", Int. J. Rock Mech. Min. Sci. 145 (2021) 104856.
[26] P.G. Asteris, P.B. Lourenço, P.C. Roussis, C.E. Adami, D.J. Armaghani, L. Cavaleri, et al., "Revealing the nature of metakaolin-based concrete materials using artificial intelligence techniques,", Construct. Build. Mater. 322 (2022) 126500.
[27] R. Trivedi, T. Singh, A. Raina, "Prediction of blast-induced flyrock in Indian limestone mines using neural networks,", J. Rock Mech. Geotech. Eng. 6 (2014) 447–454.
[28] E. Ghasemi, H. Amini, M. Ataei, R. Khalokakaei, "Application of artificial intelligence techniques for predicting the flyrock distance caused by blasting operation,", Arabian J. Geosci. 7 (2014) 193–202.
[29] H. Guo, J. Zhou, M. Koopialipoor, D. Jahed Armaghani, M. Tahir, "Deep neural network and whale optimization algorithm to assess flyrock induced by blasting,", Eng. Comput. 37 (2021) 173–186.
[30] E.T. Mohamad, D.J. Armaghani, M. Hajihassani, K. Faizi, A. Marto, "A simulation approach to predict blasting-induced flyrock and size of thrown rocks,", Electron. J. Geotech. Eng. 18 (2013) 365–374.
[31] M. Monjezi, A. Mehrdanesh, A. Malek, M. Khandelwal, "Evaluation of effect of blast design parameters on flyrock using artificial neural networks,", Neural Comput. Appl. 23 (2013) 349–356.
[32] A. Saghatforoush, M. Monjezi, R. Shirani Faradonbeh, D. Jahed Armaghani, "Combination of neural network and ant colony optimization algorithms for prediction and optimization of flyrock and back-break induced by blasting,", Eng. Comput. 32 (2016) 255–266.
[33] R. Trivedi, T. Singh, N. Gupta, Prediction of blast-induced flyrock in opencast mines using ANN and ANFIS, Geotech. Geol. Eng. 33 (2015) 875–891.
[34] B.R. Murlidhar, H. Nguyen, J. Rostami, X. Bui, D.J. Armaghani, P. Ragam, et al., "Prediction of flyrock distance induced by mine blasting using a novel Harris Hawks optimization-based multi-layer perceptron neural network,", J. Rock Mech. Geotech. Eng. 13 (2021) 1413–1427.
[35] A. Marto, M. Hajihassani, D. Jahed Armaghani, E. Tonnizam Mohamad, A.M. Makhtar, "A novel approach for blast-induced flyrock prediction based on imperialist competitive algorithm and artificial neural network,", Sci. World J. (2014) 2014.
[36] M. Monjezi, H. Amini Khoshalan, A. Yazdian Varjani, "Prediction of flyrock and backbreak in open pit blasting operation: a neuro-genetic approach,", Arabian J. Geosci. 5 (2012).
[37] M. Hasanipanah, B. Keshtegar, D.-K. Thai, N.-T. Troung, "An ANN-adaptive dynamical harmony search algorithm to approximate the flyrock resulting from blasting,", Eng. Comput. (2022) 1–13.
[38] M. Koopialipoor, A. Fallah, D.J. Armaghani, A. Azizi, E.T. Mohamad, "Three hybrid intelligent models in estimating flyrock distance resulting from blasting,", Eng. Comput. 35 (2019) 243–256.
[39] B.R. Murlidhar, D. Kumar, D. Jahed Armaghani, E.T. Mohamad, B. Roy, B.T. Pham, "A novel intelligent ELM-BBO technique for predicting distance of mine blasting-induced flyrock,", Nat. Resour. Res. 29 (2020) 4103–4120.
[40] D. Jahed Armaghani, E. Tonnizam Mohamad, M. Hajihassani, S. Alavi Nezhad Khalil Abad, A. Marto, M. Moghaddam, "Evaluation and prediction of flyrock resulting from blasting operations using empirical and computational methods,", Eng. Comput. 32 (2016) 109–121.
[41] M. Hasanipanah, R.S. Faradonbeh, D.J. Armaghani, H.B. Amnieh, M. Khandelwal, "Development of a precise model for prediction of blast-induced flyrock using regression tree technique,", Environ. Earth Sci. 76 (2017) 1–10.
[42] M. Barkhordari, D. Armaghani, P. Fakharian, "Ensemble machine learning models for prediction of flyrock due to quarry blasting,", Int. J. Environ. Sci. Technol. 19 (2022) 8661–8676.
[43] J. Ye, M. Koopialipoor, J. Zhou, D.J. Armaghani, X. He, "A novel combination of tree-based modeling and Monte Carlo simulation for assessing risk levels of flyrock induced by mine blasting,", Nat. Resour. Res. 30 (2021) 225–243.
[44] M. Yari, D.J. Armaghani, C. Maraveas, A.N. Ejlali, E.T. Mohamad, P.G. Asteris, "Several tree-based solutions for predicting flyrock distance due to mine blasting,", Appl. Sci. 13 (2023) 1345.
[45] H.N. Rad, M. Hasanipanah, M. Rezaei, A.L. Eghlim, "Developing a least squares support vector machine for estimating the blast-induced flyrock,", Eng. Comput. 34 (2018) 709–717.
[46] H. Nguyen, X.-N. Bui, Y. Choi, C.W. Lee, D.J. Armaghani, "A novel combination of whale optimization algorithm and support vector machine with different kernel functions for prediction of blasting-induced fly-rock in quarry mines,", Nat. Resour. Res. 30 (2021) 191–207.
[47] C. Li, J. Zhou, K. Du, D.J. Armaghani, S. Huang, "Prediction of flyrock distance in surface mining using a novel hybrid model of Harris hawks optimization with multi-strategies-based support vector regression,", Nat. Resour. Res. (2023) 1–29.
[48] C. Cortes, V. Vapnik, "Support-vector networks,", Mach. Learn. 20 (1995) 273–297.
[49] C. Cortes, V. Vapnik, "Support vector machine,", Mach. Learn. 20 (1995) 273–297.
[50] J.C. Platt, "12 fast training of support vector machines using sequential minimal optimization,". Advances in Kernel Methods, 1999, pp. 185–208.
[51] R.-E. Fan, P.-H. Chen, C.-J. Lin, T. Joachims, "Working set selection using second order information for training support vector machines,", J. Mach. Learn. Res. 6 (2005).
[52] M. Kloft, U. Brefeld, S. Sonnenburg, A. Zien, "Lp-norm multiple kernel learning,", J. Mach. Learn. Res. 12 (2011) 953–997.

[53] J. Bi, K. Bennett, M. Embrechts, C. Breneman, M. Song, "Dimensionality reduction via sparse support vector machines,", J. Mach. Learn. Res. 3 (2003) 1229–1243.
[54] F. Löw, U. Michel, S. Dech, C. Conrad, "Impact of feature selection on the accuracy and spatial uncertainty of per-field crop classification using support vector machines,", ISPRS J. Photogrammetry Remote Sens. 85 (2013) 102–119.
[55] M. Tanveer, K. Shubham, A regularization on Lagrangian twin support vector regression, Int. J. Machine Learn. Cybern. 8 (2017) 807–821.
[56] X. Peng, "TSVR: an efficient twin support vector machine for regression,", Neural Network. 23 (2010) 365–372.
[57] H.I. Burgan, H. Aksoy, Daily flow duration curve model for ungauged intermittent subbasins of gauged rivers, J. Hydrol. 604 (Jan 2022).
[58] D.N. Moriasi, J.G. Arnold, M.W. Van Liew, R.L. Bingner, R.D. Harmel, T.L. Veith, Model evaluation guidelines for systematic quantification of accuracy in watershed simulations,, Transac. Asabe 50 (May-Jun 2007) 885–900.
[59] Y. Li, X. Lei, N. Wang, Y. Ren, X. Jin, G. Li, et al., Study on the failure characteristics of overburden and the evolution law of seepage field in deep buried thick coal seam under aquifers, Nat. Hazards 118 (2023) 1035–1064.